Available online at www.sciencedirect.com

SCIENCE DIRECT

Developmental Brain Research 153 (2004) 97–107

DEVELOPMENTAL BRAIN RESEARCH

www.elsevier.com/locate/devbrainres

Research report

Developmental changes of transient potassium currents in large aspiny neurons in the neostriatum

Ping Deng, Zhiping Pang, Yuchun Zhang, Zao C. Xu*

Department of Anatomy and Cell Biology, Indiana University School of Medicine, 635 Barnhill Drive, MS 507, Indianapolis, IN 46202, USA

Accepted 5 August 2004
Available online 11 September 2004

Abstract

Developmental regulation of the potassium conductance is important for the maturation of neuronal excitability and the formation of functional circuitry in the central nervous system (CNS). The rapidly inactivating A-type current is a major component of the voltage-dependent outward potassium currents in the large aspiny (LA) neurons in the neostriatum. The large aspiny neurons play important roles in the function of neostriatum in physiological and pathological conditions. Whole-cell patch-clamp recording was performed on acutely dissociated neurons and brain slices to investigate the postnatal development of A-type current in the large aspiny neurons. The current density of A-type current in large aspiny neurons was the highest at postnatal 1–3 days and gradually decreased during the development with the lowest levels in adult animals. In comparison to postnatal 1–3 days, the steady-state inactivation curve shifted in depolarizing direction in mature neurons. No significant changes in the voltage dependence of steady-state activation were observed during development. Consistent with the decrease in the current density of A-type current during development, the latency to the first spike was dramatically shortened in mature large aspiny neurons. These results suggest that the decrease of rapidly inactivating A-type potassium current during development might contribute, at least in part, to the maturation of the membrane excitability of large aspiny neurons in the neostriatum.

Theme: Development and regeneration
Topic: Neurotransmitter system and channels

Keywords: Development; A-type potassium current; Membrane excitability; Whole-cell patch-clamp recording

1. Introduction

Large aspiny (LA) neurons are cholinergic interneurons in the neostriatum [3,12,48]. Morphological studies have demonstrated that LA neurons in rats have large somata (20–35 μm) with 3–5 extended primary dendrites bearing few spines [3,4]. Compared to medium-sized spiny neurons, LA neurons have relatively depolarized resting membrane potentials (about −60 mV) and show large-amplitude and long-duration afterhyperpolarizations following action potentials [2,6,35,48]. Moreover, LA neurons display a hyperpolarization-activated cation current (I_h) related sag in membrane potential during intracellular negative current injection [21,23,48]. These morphological and electrophysiological characteristics allow LA neurons to be easily distinguished from other striatal neurons. Although they only account for less than 2% of the neuronal population in the neostriatum, LA neurons exert great influences on the function of the basal ganglia by modulating the synaptic transmission of spiny projection neurons and interneurons [7,15,24,26]. Maintaining the proper neuronal excitability is essential for the function of LA neurons.

Voltage-dependent potassium currents are critical to the maintenance of neuronal excitability through the regulation

Abbreviations: ACSF, artificial cerebrospinal fluid; 4-AP, 4-aminopyradine; CNS, central nervous system; I_A, rapidly inactivating A-type potassium current; I_h, hyperpolarization-activated cation current; I_{kd}, delayed rectifier potassium current; LA, large aspiny; TEA, tetraethylammonium; TTX, tetrodotoxin

* Corresponding author. Tel.: +1 317 274 0547; fax: +1 317 278 2040.
E-mail address: zxu@anatomy.iupui.edu (Z.C. Xu).

0165-3806/$ - see front matter © 2004 Elsevier B.V. All rights reserved.
doi:10.1016/j.devbrainres.2004.08.001

of resting membrane potential, the shaping of neuronal firing patterns, the controlling of action potential frequency and the determination of neuronal responses to synaptic inputs [16,37,45]. Recent studies have shown that the rapidly inactivating A-type potassium current (I_A) is the predominant component of depolarization-activated potassium currents in LA neurons [43]. The A-type potassium channels in LA neurons are attributable to the co-expression of Kv4.2 and Kv4.1 subunits, and the Kv4.2 subunits are the major constituents of the A-type potassium channels [43,47]. Another component of the outward currents, namely the delayed rectifier potassium current (I_{kd}), is evident after inactivation of I_A [43,47]. During the postnatal development of the central nervous system (CNS), potassium conductance undergoes significant changes, which indicates that it may play important roles in the maturation of neuronal excitability as well as in the formation of functional circuitry [36]. The developmental regulation of potassium currents has been shown in many regions of the CNS, such as the cerebral cortex, the hippocampus and the cerebellar granule cells [8,11,25,28,29,41,44]. In the striatum, the developmental changes of potassium currents in spiny neurons have been elucidated [46]. In the present study, we used whole-cell patch-clamp recording techniques on acutely dissociated cells and brain slices to investigate the development of I_A in LA neurons. In brain slice preparation, the neurons are relatively intact and close to the physiological conditions. But the extended dendrites compromise the voltage clamping of the cell and might result in a space clamp error. In acutely dissociated neurons, the space clamp problem is significantly reduced by removing most of the dendrites. But the traumatic treatments during the mechanical and enzymatic procedures might have adverse effects on the physiological properties of the cell. Therefore, both techniques were used in the present study to validate the results.

2. Materials and methods

2.1. Brain slice and acute dissociation preparation

Male Wistar rats (Charles River, Wilmington, MA, USA) were used in the present study. Experimental protocols were institutionally approved in accordance with the National Institutes of Health Guide for the Care and Use of Laboratory Animals. All efforts were made to minimize the suffering and the number of animals used.

Animals at the age of postnatal days 1–3, 7–9, 14–16, 22–27, 60–90 (P1–3, P7–9, P14–16, P22–27, P60–90) were prepared for brain slices using procedures similar to those previously described [33]. Briefly, the animals were anesthetized with ketamine–HCl (80 mg/kg, i.p.) and decapitated. The brains were quickly removed and immersed in ice-cold artificial cerebrospinal fluid (ACSF), which was composed of the following (in mM): 130 NaCl, 3 KCl, 2 $CaCl_2$, 2 $MgCl_2$, 1.25 NaH_2PO_4, 26 $NaHCO_3$ and 10 glucose, pH 7.4, 295–305 mOsm/l. Transverse striatal slices of 280–300 μm thickness were cut using a vibratome (VT 1000; Leica, Nussloch, Germany) and incubated in ACSF for ≥1 h at room temperature (~24 °C) before being transferred to the recording chamber. The slice was submerged beneath the fluid surface and superfused continuously with oxygenated ACSF. The flow rate was adjusted to 2–3 ml/min. Recordings were carried out at room temperature.

Rats at the age of P1–3, P5–7, P14–16 and P25–27 were used for acute dissociation using procedures similar to those previously described [49]. In brief, rats were anesthetized and decapitated. The brains were quickly removed, iced and then blocked for slicing. The brain tissue containing neostriatum was cut in 400 μm slices while bathed in a low Ca^{2+}, HEPES-buffered solution containing (in mM): 140 Na isethionate, 2 KCl, 4 $MgCl_2$, 0.1 $CaCl_2$, 23 glucose, 15 HEPES, pH=7.4, 300–305 mosM/l. Slices were incubated at room temperature in oxygenated ACSF. Then, the slices were transferred into the low Ca^{2+} buffer and regions of striatum were dissected and placed in an oxygenated HEPES-buffered Hank's balanced salt solution containing 1–3 mg/ml protease. After 25–30 min of enzyme digestion at 35 °C, tissue was rinsed three times in the low Ca^{2+} buffer and mechanically dissociated with a graded series of fire-polished Pasteur pipettes. The cell suspension was plated onto a 12 mm cover slip (Fisherbrand Coverglass; Fisher Scientific, Pittsburgh, PA, USA), which was then placed in the recording chamber.

2.2. Whole-cell patch-clamp recording

The same procedures were applied to the recordings on brain slices and dissociated neurons. Recording electrodes were prepared from borosilicate glass (Warner Instruments, Hamden, CT, USA) using a horizontal electrode puller (P-97; Sutter Instruments, Novato, CA, USA) to produce tip openings of 1–2 μm (3–5 MΩ). Electrodes were filled with an intracellular solution containing (in mM): 145 KCl, 1 $MgCl_2$, 10 EGTA, 0.2 $CaCl_2$, 10 HEPES and 2% neurobiotin (Vector, Burlingame, CA, USA), pH 7.4, 290–295 mosM/l. Neurons were visualized with an infrared-differential interference contrast (DIC) microscope (BX 50 WI; Olympus Optical, Tokyo, Japan) and a CCD camera. Only those cells with large somata (>20 μm) were selected for recording. Whole-cell patch-clamp recordings were performed with an Axopatch 200 B amplifier (Axon Instruments, Foster City, CA, USA). After tight-seal (>1 GΩ) formation, the electrode capacitance was compensated. The cell membrane was ruptured by applying a sharp pulse of negative pressure. Immediately after establishment of whole-cell configuration, the resting membrane potential was obtained by direct reading from the amplifier. The membrane capacitance, series resistance and input resistance of the recorded neurons were measured by applying a 5 mV

(10 ms) depolarizing voltage step from a holding potential of −60 mV. The series resistance was 10–15 MΩ. Neurons with a series resistance >10% of the input resistance were discarded. The membrane capacitance reading was used as the value for whole cell capacitance. For all measurements, capacitance and series resistance compensation (60–70%) were used to minimize voltage errors. During the experiment, the membrane capacitance and series resistance were periodically monitored. Neurons with a series resistance change above 20% during the experiment were excluded from the analysis. Signals were filtered at 2 kHz and digitized at a sampling rate of 5 kHz using a data-acquisition program (Axograph 4.5; Axon Instruments).

To identify the characteristic electrophysiological responses of LA neurons, the responses induced by hyperpolarizing and depolarizing current pulses were examined in current-clamp mode. Then, the recording was switched to voltage-clamp mode to study the voltage-dependent outward potassium currents. Tetrodotoxin (TTX, 1 μM) and cadmium chloride (300 μM) were added into the perfusate to block voltage-activated Na^+ and Ca^{2+} currents, as well as Ca^{2+}-activated potassium currents. In some experiments, 4-aminopyradine (4-AP, 10 mM) and tetraethylammonium (TEA, 20 mM) were applied to examine their pharmacological effects on I_A and I_{kd}, respectively. All pharmacological agents were obtained from Sigma (St. Louis, MO, USA).

Neurobiotin was iontrophoresed into the neuron by passing depolarizing current pulses after successful recording on brain slices. The slice was then fixed overnight with 4% paraformaldehyde and incubated in 0.1% horseradish peroxidase-conjugated avidin D (Vector) in 0.01 M potassium phosphate buffer saline (pH 7.4) with 0.5% Triton X-100 for 24 h at room temperature. After the detection of peroxidase activity with 3,3′ -diaminobenzidine as chromogen, the sections were examined under a light microscope. The sections containing the labeled neurons were mounted on gelatin-coated slides for histological process. The cell bodies of the labeled LA neurons were digitized with 60× objective (BX 50 WI, Olympus Optical) and the somatic area and diameters were measured using image analysis software (Scion 1.9.2, Scion Frederick, MD, USA).

2.3. Data analysis

The current densities of I_A for each neuron were obtained by dividing the membrane capacitances from current amplitudes. The amplitudes of I_A were measured at the peak of each current (~4 ms after the onset of the command pulse). The steady-state activation or inactivation curves were established similarly to those previously reported [9]. Briefly, the conductance (G) was calculated using the following equation: $G=I/(V_m-V_k)$, where I was the current amplitude, V_m was the command potential and V_k was the reversal potential of potassium ($V_k=-98$ mV). The conductance was then normalized with respect to the maximum value and plotted as a function of the membrane potential during the test pulse. The resulting activation curves were fitted with normalized Boltzmann distribution: $G/G_{max}=1/[1+\exp(V_m-V_{1/2})/V_c]$, where G_{max} was the maximum conductance at +70 mV, $V_{1/2}$ was the membrane voltage at which the current amplitude was half-maximum and V_c was the slope factor at $V_{1/2}$. The inactivation curves were fitted with normalized Boltzmann distribution: $I/I_{max}=1/[1+\exp(V_{1/2}-V_m)/V_c$, where I_{max} was the maximum current at +70 mV.

The values were presented as means±S.E. Analysis of variance (ANOVA) followed by post-hoc Scheffe's test was used for statistical analysis (StatView 5.0; Abacus Concepts). Changes were considered significant if $P<0.05$.

3. Results

A total of 75 acutely dissociated LA neurons were recorded and analyzed in the present study. These neurons had large somata and a few dendritic processes (Fig. 1A and B). The somatic transversal area of acutely dissociated LA neurons was increased from 111.8±2.7 μm^2 at P1–3 (n=20) to 253.9±10.6 μm^2 at P14–16 (n=23, $P<0.01$), and to 282.6±11.5 m^2 at P25–27 (n=21, $P<0.01$). In addition, a total of 117 LA neurons were recorded from brain slices. Intracellular staining with neurobiotin revealed that these neurons had large somata with 3–5 primary dendrites bearing few spines. The cell bodies in early postnatal animals were smaller than those of mature ones (Fig. 1C and D). The somatic transversal area of LA neurons in brain slices at P1–3 was 123.3±8.6 μm^2 (n=23) and was significantly increased to 351.8±21.5 μm^2 at P22–27 (n=16, $P<0.01$). The soma size of dissociated LA neurons in each age group was slightly smaller than that of LA neurons in brain slices (Table 1). Spontaneous firings were observed in some adult neurons when switched to current-clamp mode. Injection of a negative current pulse produced a prominent sag following the initial hyperpolarization (Fig. 1E and F), indicating the presence of a cation current I_h [23]. Depolarizing pulses (30–100 pA) induced repetitive spiking followed by large-amplitude and long-duration afterhyperpolarization (Fig. 1E and F). These morphological and electrophysiological features are characteristic of LA neurons [24,35].

3.1. Membrane properties of LA neuron during development

The postnatal development of the membrane properties of LA neurons was investigated on brain slices by analyzing the resting membrane potential, input resistance, membrane capacitance, spike threshold, spike height and spike duration (Tables 1 and 2). The input resistance of LA neurons gradually decreased from 508.5±37.7 MΩ at P1–3 to 108.4±0.9 MΩ at P22–27 ($P<0.01$), and remained at similar levels up to P60–90. The membrane capacitance of

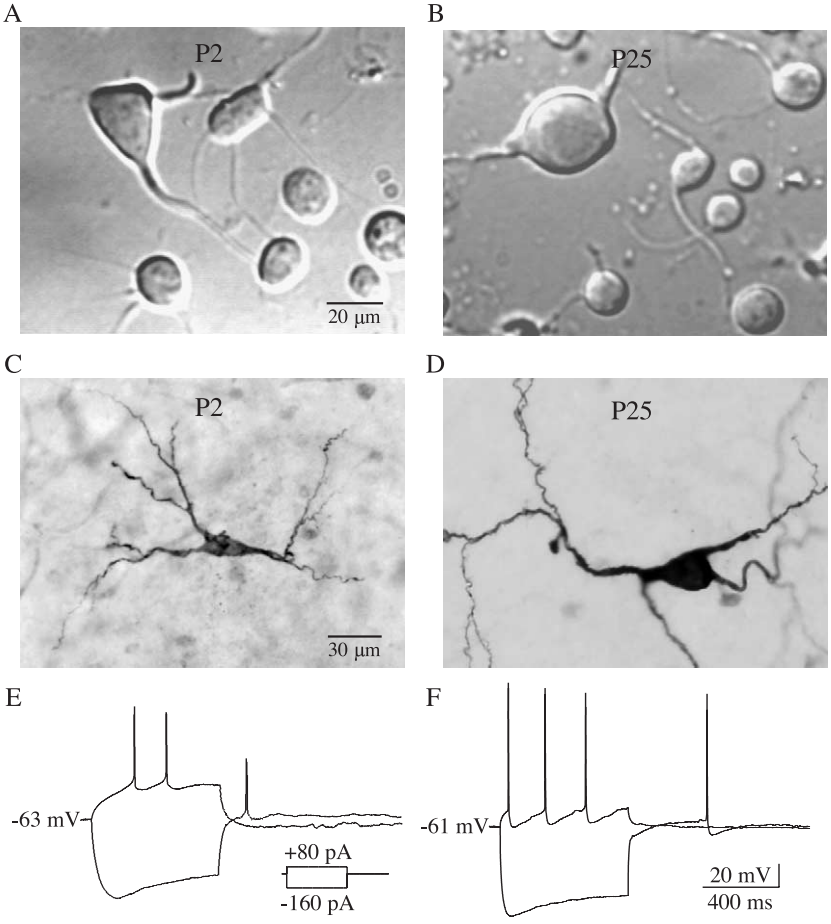

Fig. 1. Morphological and electrophysiological features of LA neurons. (A, B) Photomicrographs of acutely dissociated neurons from the neostriatum at P2 and P25, respectively. The dissociated neurons have a few short dendrites. Among neurons with smaller somata (probably medium spiny neurons), the LA neuron is easily identified due to its large soma. (C, D) Photomicrographs of intracellularly stained LA neurons from brain slices. Both neurons have large somata with three primary dendrites bearing no spines. (E, F) Representative traces showing the responses to intracellular current injection in the neurons shown in C and D, respectively. Application of a negative current pulse produced a prominent sag following the initial hyperpolarization. Depolarizing current pulse induced regular firing followed by large-amplitude and long-duration after hyperpolarization.

LA neurons gradually increased from 22.7±0.8 pF at P1–3 to 40.1±1.3 pF at P22–27 (P<0.01), which is correlated with the increase of soma size during development as shown by our morphological analysis (Table 1) as well as that of other investigators [13,38]. The spike height increased from 73.1±4.8 mV at P1–3 to 113.2±2.0 mV at P14–16 (P<0.05) and the spike duration decreased from 1.2±0.4 to 0.8±0.2 ms during the same period (P<0.05). The spike threshold showed a slight hyperpolarization with development and the resting membrane potential of LA neurons remained at similar levels during postnatal development.

3.2. Developmental changes of I_A in LA neurons

To induce voltage-dependent outward potassium currents, the membrane potentials of LA neurons were held at −60

Table 1
Developmental changes of somatic size and capacitance of LA neuron

	Dissociated cell				Brain slice			
	P1–3 (n=20)	P5–7 (n=19)	P14–16 (n=23)	P25–27 (n=21)	P1–3 (n=23)	P7–9 (n=12)	P14–16 (n=13)	P22–27 (n=16)
Area (μm^2)	112±2.7	156±9.2*	254±10.6**	283±11.5**	123±8.6	206±14.6*	268±25.2**	352±21.5**
Long axis (μm)	15±0.3	18±0.6	22±0.9**	23±0.7**	20±0.9	22±1.2	27±1.7*	31±1.7**
Short axis (μm)	10±0.3	11±0.5	15±0.4*	16±0.8*	8±0.4	12±0.7**	13±0.6**	14±0.7**
Capacitance (pF)	12±0.5	16±0.9	29±1.4**	30±1.2**	23±0.8	33±1.0*	38±0.9**	40±1.3**

Values are mean±S.E., with number of neurons in parentheses. Comparing to P1–3.
* P<0.05.
** P<0.01.

Table 2
Membrane properties of striatal LA neurons during development

	P1–3 (n=14)	P7–9 (n=21)	P14–16 (n=27)	P22–27 (n=19)	P60–90 (n=30)
RMP (mV)	−59.2±1.6	−59.4±1.0	−63.7±1.0	−60.0±0.9	−58.4±0.7
R_{in} (MΩ)	508.5±37.7	288.4±14.9*	146.1±9.8*	108.4±0.9*	118.3±5.2*
T_{con} (ms)	69.2±13.3	48.5±6.4*	38.4±4.8*	31.2±3.7*	30.7±4.1*
SpkT (mV)	−44.9±1.0	−44.1±1.7	−48.9±0.6	−48.9±1.5	−48.9±2.7
SpkH (mV)	73.1±4.8	78.1±4.3	113.2±2.0*	107.3±3.2*	100.9±5.1*
SpkD (ms)	1.2±0.4	1.1±0.3	0.8±0.2*	0.8±0.1*	0.9±0.3*

Values are mean±S.E., with number of neurons in parentheses. RMP, resting membrane potential; R_{in}, input resistance; T_{con}, time constant, measured from transients of hyperpolarzing pulses (−60 pA, 600 ms); SpkT, spike threshold, measured at the beginning of the upstroke of the first action potential; SpkH, spike height, measured from the resting membrane potential; SpkD, spike duration, measured at the half-amplitude of the first action potential.

* Comparing to P1–3, P<0.05.

mV and command voltage pulses (from −80 to +70 mV, 10 mV increment, 400 ms) were applied following a conditioning voltage step of 300 ms at −120 mV (protocol 1) (Fig. 2A). The evoked potassium currents became apparent at about −50 mV and the amplitude increased with more depolarizing voltage pulses. It has been shown that the outward potassium current in LA neurons mainly consists of a transient current and a sustained current [43]. To isolate the sustained current, the transient current was inactivated by a 100-ms pre-pulse at +10 mV following a conditioning voltage step (−120 mV, 200 ms). The sustained current was then elicited by depolarizing voltage pulses (protocol 2) (Fig. 2B). The transient current was isolated by subtracting the current evoked by protocol 2 from the current evoked by protocol 1 (Fig. 2C). Bath application of 20 mM TEA significantly reduced the amplitude of the sustained current. Additional application of 10 mM 4-AP selectively blocked the transient current (Fig. 2D). These results indicated that the sustained current resembles I_{kd} and the transient current resembles I_A [9,25,45]. Representative recordings of outward potassium currents from brain slices at different ages are presented in Fig. 2E.

Because the changes in current amplitudes might result from the cell volume change during development, current density was used to analyze the development of I_A. Comparison of the current density curve of I_A in acutely

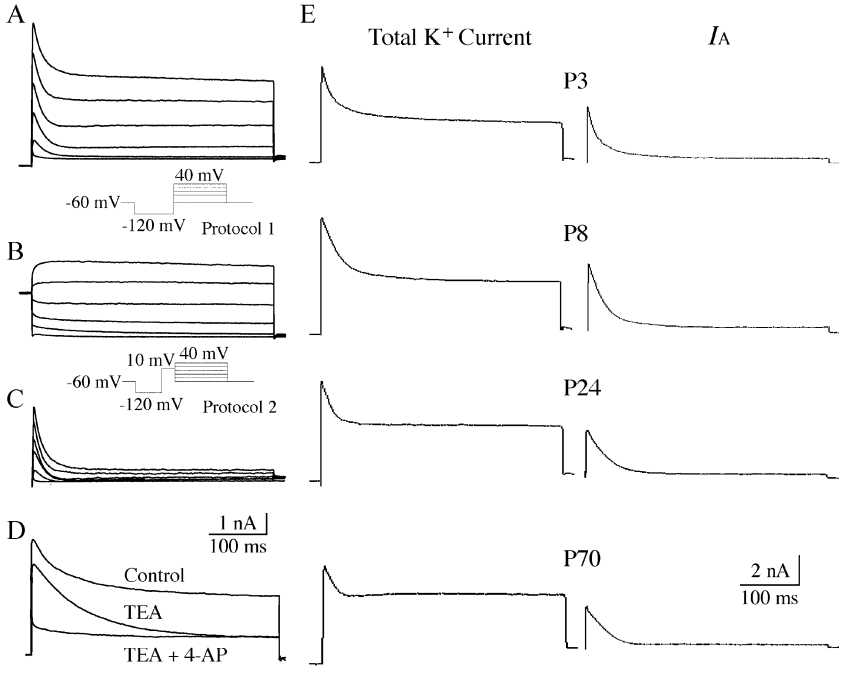

Fig. 2. The components of potassium currents in LA neurons. (A) Outward potassium currents were evoked from a LA neuron at P16 with protocol 1 (inset). (B) Sustained potassium currents were isolated from the same neuron by the inactivation of rapidly inactivating potassium currents using protocol 2 (inset). (C) The rapidly inactivating potassium currents were isolated by subtracting the sustained currents (B) from the total potassium currents (A). (D) Pharmacological effects of specific potassium channel blockers on these currents. Bath application of 20 mM TEA significantly reduced the sustained current suggesting that it is a delayed rectifier potassium current (I_{kd}). An additional application of 10 mM 4-AP selectively blocked the rapidly inactivating current suggesting that it is an A-type potassium current (I_A). Traces were recorded from a LA neuron at P22 with a command voltage of +20 mV (protocol 1). (E) Representative traces recorded from LA neurons at different ages.

dissociated neurons indicates that the current density significantly decreased with development ($P<0.01$, Fig. 3A). As shown in Fig. 3B, the amplitude of I_A increased during development but the current density of I_A significantly decreased with age. At a depolarizing voltage of +30 mV, the current density decreased from 194.3±8.3 pA/pF at P1–3 ($n=23$) to 113.6±7.8 pA/pF at P25–27 ($n=18$, $P<0.01$). The developmental changes in the voltage dependence of I_A were investigated by comparing the activation and inactivation curves at different postnatal stages. No significant difference in the $V_{1/2}$ and V_c of the activation curve was found in dissociated LA neurons during development (Fig. 3C, Table 3). The steady-state inactivation properties of I_A were determined by measuring the current availability following 2 s pre-pulse steps of voltages between −120 and 0 mV with a testing pulse of +70 mV (Fig. 3D). While there were no significant changes in the V_c of the inactivation curve during development, the $V_{1/2}$ of the inactivation curve shifted from −87.4±1.3 mV at P1–3 ($n=23$) to −71.3±1.0 mV at P25–27 ($n=18$, $P<0.01$, Fig. 3D, Table 3). Based on the activation curve, the test pulse of +30 mV that reaches the plateau region of the curve (Fig.

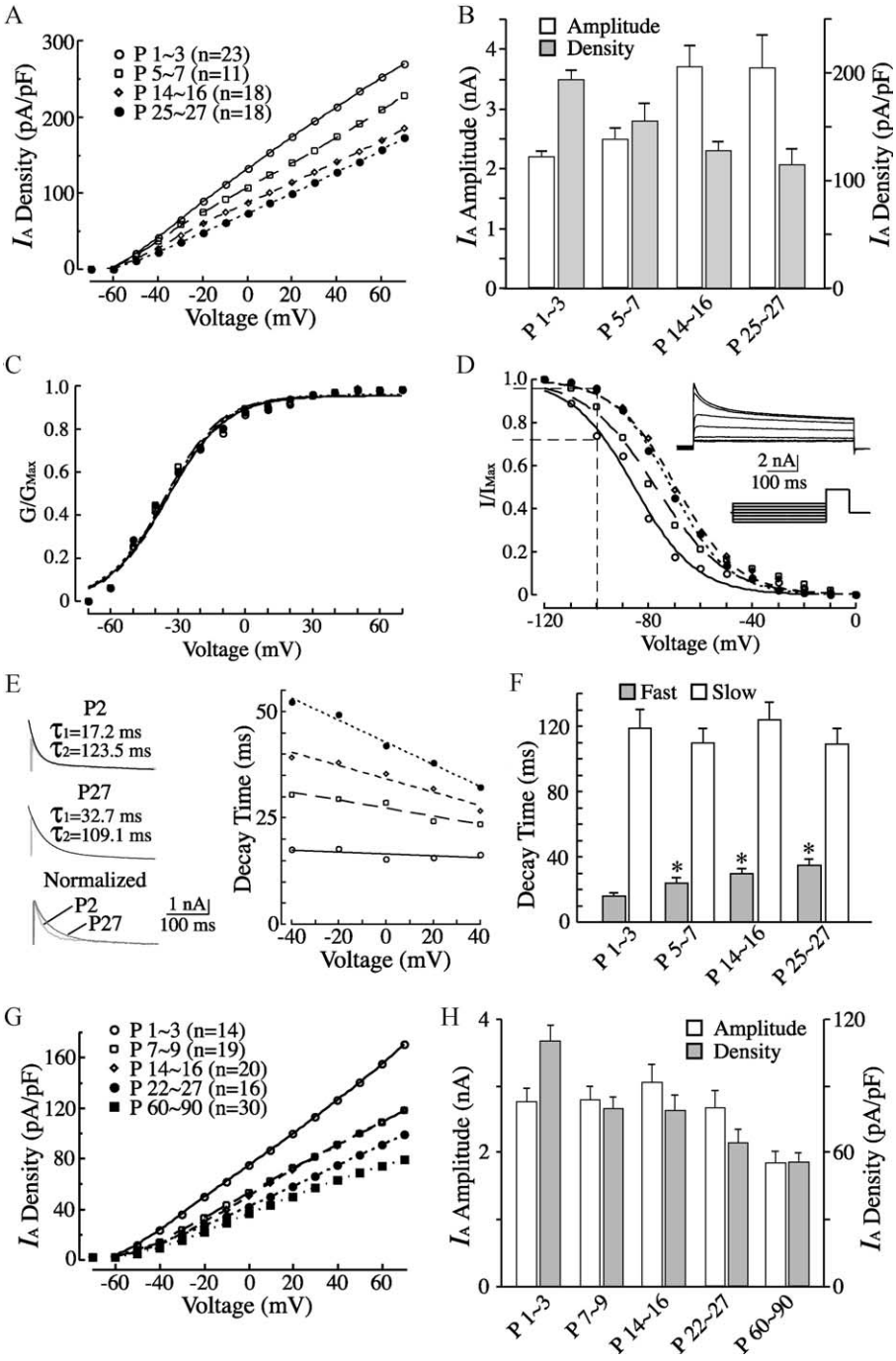

Table 3
Developmental changes in the voltage dependence of activation and inactivation of I_A in acutely dissociated cells

	P1–3 (n=23)	P5–7 (n=11)	P14–16 (n=18)	P25–27 (n=18)
$V_{1/2}$ (Act), mV	−33.6±1.4	−32.7±1.3	−33.2±2.5	−34.8±3.3
Vc (Act), mV	12.5±0.7	13.4±0.5	12.1±1.1	14.1±2.2
$V_{1/2}$ (Inact), mV	−87.4±1.3	−77.2±2.3*	−70.4±1.9*	−71.3±1.0*
Vc (Inact), mV	9.9±0.6	10.1±1.1	10.2±0.9	10.3±0.6

Values are mean±S.E., with number of neurons in parentheses. $V_{1/2}$, the potential of half-maximal activation (Act) or inactivation (Inact); Vc, proportional to the slope at $V_{1/2}$.

* Comparing to P1–3, P<0.01.

3C) was expected to activate the maximum number of A-type channels at all ages. Therefore, the I_A elicited by the test pulses of +30 mV was used to compare the developmental changes. As shown in Fig. 3B, the amplitude of I_A slightly changed during development but the current density of I_A decreased with age due to the increase of cell capacitance. To further characterize the postnatal changes in the kinetics of I_A in LA neurons, the decay time constant of I_A was examined. The decay time constant was derived from a double-exponential fitting to the falling phase of I_A. The time constant of the fast component increased with development (Fig. 3E). At +30 mV command voltage, the fast time constant was 17.5±1.1 ms at P1–3 (n=17) and gradually increased to 36.3±2.8 ms at P25–27 (n=18, P<0.01). In addition, the fast time constant at P1–3 showed no significant changes with the increment of the command voltage, whereas at later developmental stages, the decay time constant became smaller according to the increment of the command voltage (Fig. 3E). The slope of the voltage-decay curve in Fig. 3E was −0.051±0.012 ms/mV at P1–3 (n=17) and decreased remarkably to −0.32±0.037 ms/mV at P25–27 (n=18, P<0.01). These data indicate that the voltage dependence of the decay time of I_A is developmentally regulated. In contrast to the fast component, the slow time constant showed no significant changes with the increase of the command voltages and no significant change during development was observed (Fig. 3F).

The current density of I_A in LA neurons from brain slices was also compared during development using the same protocols as those in the dissociated cell preparation. As shown in Fig. 3G, the current density of I_A decreased during development. At a depolarizing voltage of +30 mV, the current density decreased from 110.8±6.7 pA/pF at P1–3 (n=14) to 54.9±4.0 pA/pF at P60–90 (n=30, P<0.01, Fig. 3H). These findings were coincident with the results obtained from the dissociated cells.

A recent study by Hattori et al has reported that the A-type potassium current recorded from acutely dissociated LA neurons was up-regulated with age [17]. The shift of the inactivation curve in a hyperpolarizing direction in young LA neurons might be one of the reasons for the conflicting results between the present study and Hattori et al. (2003). The conditioning pre-pulse of −120 mV was used in the present study to remove inactivation of I_A channels, whereas the conditioning pre-pulse of −100 mV was used by Hattori and his colleagues. The pre-pulse of −100 mV removed most of the inactivated channels in adult neurons but only removed ~75% of the inactivated channels in neurons of P1–3 (dotted line, Fig. 3D). To examine the effects of different conditioning pre-pulses on A-type currents in LA neurons, the recordings were performed on the same dissociated LA neuron using the pre-pulses of −120 and −100 mV, respectively (Fig. 4A). As shown in Fig. 4B–D, at P1–3, the amplitude and current density of I_A

Fig. 3. Developmental changes of I_A in LA neurons. (A) Plotting showing the current density of I_A in acutely dissociated LA neurons as a function of command voltage at different ages. The current density increased with the increment of command voltages. Compared with the values at P1–3, the current density gradually decreased during development (P<0.01). (B) Histograms showing the developmental changes of amplitude and current density of I_A in acutely dissociated LA neurons evoked at command voltage of +30 mV. The amplitude of I_A increased during development but the current density gradually decreased from P1–3 to P25–27. (C) Voltage dependence of activation of I_A in acutely dissociated LA neurons at different age groups. No significant changes in activation curve were observed during development. (D) The steady-state inactivation of I_A in dissociated neurons during development. The inactivation curve shifted in depolarizing direction during development (P<0.01). At −100 mV, more than 95% of the channels are available at P25–27, whereas less than 75% of the channels are available at P1–3 (dotted line). A representative recording of the inactivation of I_A was shown in the inset. (E, F) Comparison of decay time of I_A during development. (E) Development of the time constant of the fast component. Left panel: examples of double-exponential fittings of the inactivating phase of I_A from P2 and P27 LA neurons elicited with a command voltage of +30 mV. The two traces are normalized and superimposed to show the difference in decay time. Right panel: plotting of decay time constant of I_A as a function of command voltage. The decay time constant at P1–3 showed no significant change with the increase of command voltages, whereas the decay time constant in more mature animals became significantly smaller with the increment of command voltages. The symbols for different development groups in A apply to C, D and E. (F) Developmental change of the time constant of the fast and slow component. The value was measured at +30 mV command voltage. The fast component was significantly increased during development, while the slow component remained unchanged. (G) Plotting showing the current density of I_A in brain slice as a function of command voltage at different ages. The current density increased with the increment of command voltages. Compared to the value at P1–3, the current density gradually decreased during development (P<0.01), with the lowest density value in animals of P60–90. (H) Histograms showing the developmental changes of amplitude and current density of I_A in brain slice evoked by command voltage of +30 mV. The amplitude of I_A slightly increased at P14–16 and decreased after P22–27. However, the current density gradually decreased due to the dramatic increase of cell capacitance during development. *P<0.01.

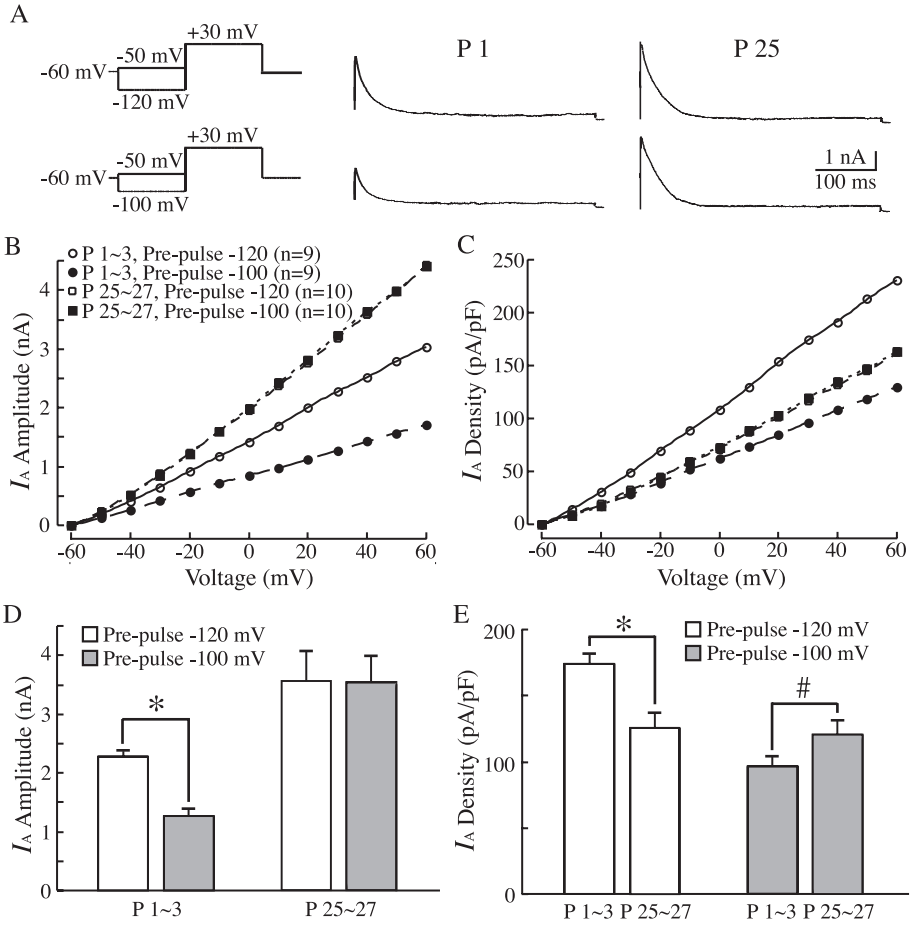

Fig. 4. The effects of the different conditioning pre-pulses on I_A. (A) Representative traces of I_A recorded from dissociated LA neurons at P1 or P25. Protocols were shown in the left panel. (B, C) Plotting showing the effects of pre-pulse of −120 and −100 mV on the amplitude (B) and current density (C) of I_A evoked by different command voltages during development. The amplitude and current density in mature neurons are about the same using either pre-pulse but the amplitude of current density of neurons at P1–3 are significantly greater with pre-pulse of −120 mV than those with pre-pulse of −100 mV. The symbols for different development groups in B apply to C. (D) The amplitude of I_A evoked from the same neurons by depolarizing voltage step of +30 mV with different pre-pulses. At P1–3, the amplitude of I_A with pre-pulse of −100 mV was significantly smaller than that with pre-pulse of −120 mV. The amplitude of I_A was about the same with pre-pulse of −100 or −120 mV at P25–27. (E) The comparison of current density of I_A evoked by command voltage step of +30 mV in different age groups. With pre-pulse of −120 mV, the current density of I_A was significantly decreased with age. In contrast, with pre-pulse of −100 mV, the current density was significantly increased with age. $^{*}P<0.01$, $^{\#}P<0.05$.

evoked by the pre-pulse of −120 mV (2.28±0.08 nA and 174.2±7.1 pA/pF, at +30 mV, n=9) was significantly greater than those evoked by the pre-pulse of −100 mV (1.27±0.11 nA and 96.4±7.7 pA/pF, $P<0.01$), whereas no difference in the amplitude and current density of I_A at P25–27 was detected between the pre-pulses of −120 and −100 mV (3.18±0.29 vs. 3.24±0.28 nA, 116.8±9.1 vs. 119.3±9.0 pA/pF, n=10). Therefore, the current density of I_A in

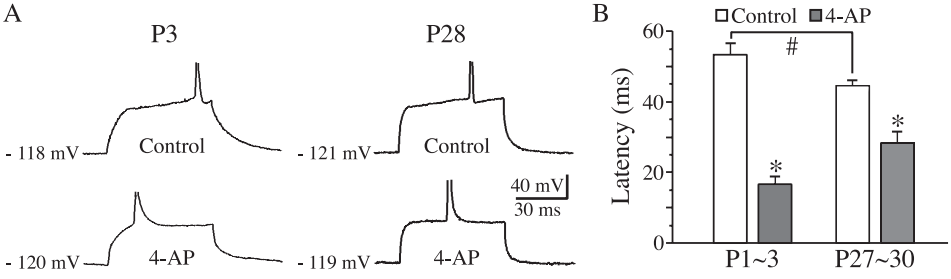

Fig. 5. Developmental changes of the latency to the first spike in LA neurons. (A) Representative recordings showing different latency in LA neurons at P3 and P28, before and after application of 10 mM 4-AP. The spikes were truncated. (B) Pooled data of the latency to the first spike in LA neurons at P1–3 (n=9) and P27–30 (n=11). Compared to P1–3, the latency was significantly shortened in mature neurons. Application of 10 mM 4-AP dramatically shortened 36.8 and 16.1 ms of the latency at P1–3 and in mature neurons. $^{*}P<0.01$, $^{\#}P<0.05$.

dissociated LA neurons with the conditioning pre-pulse of −120 mV decreased significantly from P1–3 to P25–27 as demonstrated in the present study, while the current density of I_A with the conditioning pre-pulse of −100 mV increased significantly with age as indicated by Hattori et al. (Fig. 4E).

Because A-type currents are important for determining the latency to the first spike and neuronal excitability, current-clamp recordings were carried out to examine the latency to the first spike in LA neurons in brain slices at P1–3 and in mature animals (P27–30). The neurons were held at near −120 mV to remove the inactivation of I_A, and a small depolarizing current pulse (60 ms) was applied to elicit a single action potential. The latency was measured from the onset of the current injection to the peak of the action potential. As shown in Fig. 5, the latency was significantly shortened from 53.4±3.3 ms at P1–3 (n=9) to 44.6±1.5 ms in mature neurons (n=11, P<0.05). Moreover, application of 10 mM 4-AP shortened the latency of 36.8±3.1 ms (n=9) and 16.1±2.2 ms (n=11) at P1–3 and in mature neurons, respectively (P<0.01). These results indicate that the excitability of the LA neuron increases with age, which might result from the decrease of current density of I_A.

4. Discussion

Spiny neurons in the neostriatum undergo profound changes during development [32,46]. However, studies on the postnatal development of potassium currents in LA neurons are less extensive. The present study demonstrated that the current density of I_A gradually decreased during development. In comparison with P1–3, the latency to the first spike was significantly reduced in the mature LA neurons. These results suggest that the decrease of I_A during development might contribute, at least in part, to the increase of excitability in LA neurons.

In the present study, acutely dissociated neurons and brain slices were used to study the developmental changes of I_A in LA neurons using similar experimental procedures and protocols. The limitation of whole-cell voltage-clamp recording on neurons in brain slices is the space clamp problem due to the existence of extended dendrites and axons. The amplitude and kinetics of the current might be distorted by the currents from the regions where the voltages have not been fully controlled by commands. Dissociated neurons are the better choice in this regard because most of the processes have been removed. However, the mechanical and enzymatic treatment during dissociation might compromise the normal function of the channel. The traumatic effects become more obvious in neurons from adult animals. In the present study, the decrease of I_A in LA neurons with maturation has been observed with both preparations. Some minor differences have also been noticed. For instance, the somatic areas of dissociated neurons are slightly smaller than those of neurons in slices across all age groups. This might result from the contraction of the cell bodies in acutely dissociated neurons because of the disappearance of the stretching forces imposed by the processes and the adjacent tissues. The current amplitude in more mature neurons in dissociated neurons is slightly larger that that in brain slices while the current amplitude in younger neurons is about the same in these two preparations. This might simply stem from the more severe space clamp problem in brain slices from more mature animals because more dendrites have developed with age. Despite these differences, the consistent results from both preparations indicate that the current density of A-type potassium current in LA neurons decreases during development.

The present study has shown a significant decrease in current density of I_A in LA neurons during development. This finding coincides with the developmental changes of I_A in other neurons, such as pyramidal neurons and dentate granule cells in the hippocampus [1,25] and Cajal-Retzius cells in the cortex [31]. In contrast, other studies have indicated that the expression of I_A is up-regulated during development. For example, compared with early postnatal levels, there is a pronounced increase of I_A in cerebellar granule neurons [41], hypothalamic neurons [42] and superior cervical ganglion neurons [30] after maturation. These results suggest that the developmental regulation of I_A varies among different neuronal types.

In contrast to our findings, a recent study using acutely dissociated cells has shown that the A-type current in LA neurons up-regulated with age [17]. One possible factor that might contribute to the discrepancy between the two studies is the difference in conditioning pre-pulses to remove inactivation of A-type channels. Pre-pulses of −120 mV were used in the present study while pre-pulses of −100 mV were used by Hattori et al. Based on our observation (Table 3) and those of Hattori et al (2003), the $V_{1/2}$ of inactivation curve in dissociated LA neurons at P1–3 is approximately −90 mV, and the pre-pulse of −100 mV cannot fully remove the inactivated A-type channels in young LA neurons (~75% as shown in Fig. 3D), which results in a smaller amplitude of I_A. It is conceivable that the increase of current density of I_A during development as reported by Hattori et al might be due to underestimation of the I_A in the early postnatal neurons. Comparison of the amplitude and current density of I_A in the same neuron with different conditioning pre-pulses (Fig. 4) has unequivocally demonstrated that this is indeed the case. Recently, the rundown of A-type currents in LA neurons during recording has been reported [18]. Both activation and inactivation curves shift towards hyperpolarized potentials during rundown. The rundown can be suppressed by highly hyperpolarized pre-pulse (−140 mV) and intracellular ATP (2 mM). In the present study, ATP was not included in the intracellular solution, which might influence the voltage dependence of the activation and inactivation of I_A. However, the rundown should not invalidate the results of the present study because the comparison was based on the data collected under the same experimental conditions.

The mechanisms underlying the developmental regulation of I_A are under active investigation. Several factors, such as the developmental changes in the voltage dependence and the kinetics of potassium channels, might be related to the reduction of I_A [11,40,41]. Another possible contributing factor to the decrease of the current density of I_A is the developmental changes of channel composition and distribution in LA neurons. A-type currents in LA neurons are attributable to co-expression of Kv4.2 and Kv4.1 subunits [43] and Kv4.2 mRNA abundance is linearly related to the I_A amplitude [47]. Studies have demonstrated that the subcellular location of Kv4.2 protein shifts from somata to dendrites as development proceeds [39,40]. It is conceivable that the soma-dendritic translocation of Kv4.2 subunits during development might also contribute to the decrease of I_A in mature LA neurons.

Voltage-dependent potassium currents play important roles in regulating membrane excitability. I_A has been implicated in determining the latency to first spike, the threshold and repolarization of action potentials [20,37,45]. In the present study, the latency to the first spike was dramatically shortened in mature LA neurons compared to that of P1–3. In addition, the spike threshold of LA neurons was slightly decreased during development (from ~−44 mV at early postnatal days to ~−49 mV at more mature stages, Table 2). These developmental changes might result from the down-regulation of I_A as observed during the same period of time. The shorter latency and the reduction of spike threshold would certainly increase the probability of action potential generation and change the repetitive firing pattern of LA neurons [10]. These changes could have significant impacts on the development and function of the basal ganglia. It has been well established that the neuronal activity and excitability determine the neuronal differentiation and synaptogenesis during development [27,36,41]. LA neurons are cholinergic in nature and make postsynaptic connections within the striatum mainly on spiny neurons [3,22,48]. By activating muscarinic receptors, LA neurons reduce the amplitudes of fast EPSPs [5,14] and regulate the calcium and potassium currents in spiny neurons [19,34]. Thus, the alterations in the excitability and firing pattern of LA neurons during development could influence the activity of the spiny neurons that are the major projection neurons of the neostriatum.

Acknowledgements

This work was supported by NIH Grant NS 38053. P.D. and Z.P. are recipients of American Heart Association postdoctoral fellowship (0225549Z, 0425689Z and 0120566Z). We thank Drs. Z. Yan and X.X. Chi for technical advices during this study, and Miss Michelle Werner for the secretarial assistance.

References

[1] H. Beck, E. Ficker, U. Heinemann, Properties of two voltage-activated potassium currents in acutely isolated juvenile rat dentate gyrus granule cells, J. Neurophysiol. 68 (1992) 2086–2099.
[2] B.D. Bennett, J.C. Callaway, C.J. Wilson, Intrinsic membrane properties underlying spontaneous tonic firing in neostriatal cholinergic interneurons, J. Neurosci. 20 (2000) 8493–8503.
[3] J.P. Bolam, C.A. Ingham, A.D. Smith, The section-Golgi-impregnation procedure-3. Combination of Golgi-impregnation with enzyme histochemistry and electron microscopy to characterize acetylcholinesterase-containing neurons in the rat neostriatum, Neuroscience 12 (1984) 687–709.
[4] J.P. Bolam, B.H. Wainer, A.D. Smith, Characterization of cholinergic neurons in the rat neostriatum. A combination of choline acetyltransferase immunocytochemistry, Golgi-impregnation and electron microscopy, Neuroscience 12 (1984) 711–718.
[5] P. Calabresi, N.B. Mercuri, G. Bernardi, Chemical modulation of synaptic transmission in the striatum, Prog. Brain Res. 99 (1993) 299–308.
[6] P. Calabresi, D. Centonze, A. Pisani, G. Bernardi, Metabotropic glutamate receptors and cell-type-specific vulnerability in the striatum: implication for ischemia and Huntington's disease, Exp. Neurol. 158 (1999) 97–108.
[7] P. Calabresi, D. Centonze, P. Gubellini, G.A. Marfia, A. Pisani, G. Sancesario, G. Bernardi, Synaptic transmission in the striatum: from plasticity to neurodegeneration, Prog. Neurobiol. 61 (2000) 231–265.
[8] W.E. Cameron, P.A. Nunez-Abades, I.A. Kerman, T.M. Hodgson, Role of potassium conductances in determining input resistance of developing brain stem motoneurons, J. Neurophysiol. 84 (2000) 2330–2339.
[9] X.X. Chi, Z.C. Xu, Differential changes of potassium currents in CA1 pyramidal neurons after transient forebrain ischemia, J. Neurophysiol. 84 (2000) 2834–2843.
[10] J.A. Connor, C.F. Stevens, Voltage clamp studies of a transient outward membrane current in gastropod neural somata, J. Physiol. 213 (1971) 21–30.
[11] P.F. Costa, A.I. Santos, M.A. Ribeiro, Potassium currents in acutely isolated maturing rat hippocampal CA1 neurones, Brain Res. Dev. Brain Res. 83 (1994) 216–223.
[12] M. DiFiglia, Synaptic organization of cholinergic neurons in the monkey neostriatum, J. Comp. Neurol. 255 (1987) 245–258.
[13] M. Difiglia, P. Pasik, T. Pasik, Early postnatal development of the monkey neostriatum: a Golgi and ultrastructural study, J. Comp. Neurol. 190 (1980) 303–331.
[14] H.U. Dodt, U. Misgeld, Muscarinic slow excitation and muscarinic inhibition of synaptic transmission in the rat neostriatum, J. Physiol. 380 (1986) 593–608.
[15] E. Galarraga, S. Hernandez-Lopez, A. Reyes, I. Miranda, F. Bermudez-Rattoni, C. Vilchis, J. Bargas, Cholinergic modulation of neostriatal output: a functional antagonism between different types of muscarinic receptors, J. Neurosci. 19 (1999) 3629–3638.
[16] L. Gan, L.K. Kaczmarek, When, where, and how much? Expression of the Kv3.1 potassium channel in high-frequency firing neurons, J. Neurobiol. 37 (1998) 69–79.
[17] S. Hattori, F. Murakami, W.J. Song, Quantitative relationship between kv4.2 mRNA and A-type K+ current in rat striatal cholinergic interneurons during development, J. Neurophysiol. 90 (2003) 175–183.
[18] S. Hattori, F. Murakami, W.J. Song, Rundown of a transient potassium current is attributable to changes in channel voltage dependence, Synapse 48 (2003) 57–65.
[19] A.R. Howe, D.J. Surmeier, Muscarinic receptors modulate N-, P-, and L-type Ca^{2+} currents in rat striatal neurons through parallel pathways, J. Neurosci. 15 (1995) 458–469.

[20] D.J. Jagger, G.D. Housley, A-type potassium currents dominate repolarisation of neonatal rat primary auditory neurones in situ, Neuroscience 109 (2002) 169–182.
[21] Z.G. Jiang, R.A. North, Membrane properties and synaptic responses of rat striatal neurones in vitro, J. Physiol. 443 (1991) 533–553.
[22] Y. Kawaguchi, Large aspiny cells in the matrix of the rat neostriatum in vitro: physiological identification, relation to the compartments and excitatory postsynaptic currents, J. Neurophysiol. 67 (1992) 1669–1682.
[23] Y. Kawaguchi, Physiological, morphological, and histochemical characterization of three classes of interneurons in rat neostriatum, J. Neurosci. 13 (1993) 4908–4923.
[24] Y. Kawaguchi, C.J. Wilson, S.J. Augood, P.C. Emson, Striatal interneurones: chemical, physiological and morphological characterization, Trends Neurosci. 18 (1995) 527–535.
[25] R. Klee, E. Ficker, U. Heinemann, Comparison of voltage-dependent potassium currents in rat pyramidal neurons acutely isolated from hippocampal regions CA1 and CA3, J. Neurophysiol. 74 (1995) 1982–1995.
[26] T. Koos, J.M. Tepper, Inhibitory control of neostriatal projection neurons by GABAergic interneurons, Nat. Neurosci. 2 (1999) 467–472.
[27] P. Legendre, D.A. Poulain, J.D. Vincent, A study of ionic conductances involved in plateau potential activity in putative vasopressinergic neurons in primary cell culture, Brain Res. 457 (1988) 386–391.
[28] S.Q. Liu, L.K. Kaczmarek, Depolarization selectively increases the expression of the Kv3.1 potassium channel in developing inferior colliculus neurons, J. Neurosci. 18 (1998) 8758–8769.
[29] J.L. Massengill, M.A. Smith, D.I. Son, D.K. O'Dowd, Differential expression of K4-AP currents and Kv3.1 potassium channel transcripts in cortical neurons that develop distinct firing phenotypes, J. Neurosci. 17 (1997) 3136–3147.
[30] S. McFarlane, E. Cooper, Postnatal development of voltage-gated K currents on rat sympathetic neurons, J. Neurophysiol. 67 (1992) 1291–1300.
[31] J.M. Mienville, I. Maric, D. Maric, J.R. Clay, Loss of IA expression and increased excitability in postnatal rat Cajal-Retzius cells, J. Neurophysiol. 82 (1999) 1303–1310.
[32] U. Misgeld, H.U. Dodt, M. Frotscher, Late development of intrinsic excitation in the rat neostriatum: an in vitro study, Brain Res. 392 (1986) 59–67.
[33] Z.P. Pang, P. Deng, Y.W. Ruan, Z.C. Xu, Depression of fast excitatory synaptic transmission in large aspiny neurons of the neostriatum after transient forebrain ischemia, J. Neurosci. 22 (2002) 10948–10957.
[34] J.C. Pineda, E. Galarraga, J. Bargas, M. Cristancho, J. Aceves, Charybdotoxin and apamin sensitivity of the calcium-dependent repolarization and the afterhyperpolarization in neostriatal neurons, J. Neurophysiol. 68 (1992) 287–294.
[35] A. Pisani, P. Bonsi, D. Centonze, P. Calabresi, G. Bernardi, Activation of D2-like dopamine receptors reduces synaptic inputs to striatal cholinergic interneurons, J. Neurosci. 20 (2000) RC69.
[36] A.B. Ribera, N.C. Spitzer, Developmental regulation of potassium channels and the impact on neuronal differentiation, Ion Channels 3 (1992) 1–38.
[37] B. Rudy, Diversity and ubiquity of K channels, Neuroscience 25 (1988) 729–749.
[38] B. Schlosser, G. Klausa, G. Prime, G. Ten Bruggencate, Postnatal development of calretinin- and parvalbumin-positive interneurons in the rat neostriatum: an immunohistochemical study, J. Comp. Neurol. 405 (1999) 185–198.
[39] M. Sheng, M.L. Tsaur, Y.N. Jan, L.Y. Jan, Subcellular segregation of two A-type K+ channel proteins in rat central neurons, Neuron 9 (1992) 271–284.
[40] R. Shibata, Y. Wakazono, K. Nakahira, J.S. Trimmer, K. Ikenaka, Expression of Kv3.1 and Kv4.2 genes in developing cerebellar granule cells, Dev. Neurosci. 21 (1999) 87–93.
[41] R. Shibata, K. Nakahira, K. Shibasaki, Y. Wakazono, K. Imoto, K. Ikenaka, A-type K+ current mediated by the Kv4 channel regulates the generation of action potential in developing cerebellar granule cells, J. Neurosci. 20 (2000) 4145–4155.
[42] S.K. Sikdar, P. Legendre, B. Dupouy, J.D. Vincent, Maturation of a transient outward potassium current in mouse fetal hypothalamic neurons in culture, Neuroscience 43 (1991) 503–511.
[43] W.J. Song, T. Tkatch, G. Baranauskas, N. Ichinohe, S.T. Kitai, D.J. Surmeier, Somatodendritic depolarization-activated potassium currents in rat neostriatal cholinergic interneurons are predominantly of the A type and attributable to coexpression of Kv4.2 and Kv4.1 subunits, J. Neurosci. 18 (1998) 3124–3137.
[44] I. Spigelman, L. Zhang, P.L. Carlen, Patch-clamp study of postnatal development of CA1 neurons in rat hippocampal slices: membrane excitability and K+ currents, J. Neurophysiol. 68 (1992) 55–69.
[45] J.F. Storm, Potassium currents in hippocampal pyramidal cells, Prog. Brain Res. 83 (1990) 161–187.
[46] D.J. Surmeier, A. Stefani, R.C. Foehring, S.T. Kitai, Developmental regulation of a slowly-inactivating potassium conductance in rat neostriatal neurons, Neurosci. Lett. 122 (1991) 41–46.
[47] T. Tkatch, G. Baranauskas, D.J. Surmeier, Kv4.2 mRNA abundance and A-type K(+) current amplitude are linearly related in basal ganglia and basal forebrain neurons, J. Neurosci. 20 (2000) 579–588.
[48] C.J. Wilson, H.T. Chang, S.T. Kitai, Firing patterns and synaptic potentials of identified giant aspiny interneurons in the rat neostriatum, J. Neurosci. 10 (1990) 508–519.
[49] Z. Yan, D.J. Surmeier, D5 dopamine receptors enhance Zn^{2+}-sensitive GABA(A) currents in striatal cholinergic interneurons through a PKA/PP1 cascade, Neuron 19 (1997) 1115–1126.